

**Supporting Information**

**Blue Light Emitting Self-healable Graphene**

**Quantum Dots Embedded Hydrogels**

Sagar Biswas, Dnyaneshwar B. Rasale and Apurba K. Das\*

Discipline of Chemistry, Indian Institute of Technology Indore, Indore, 452020, India

E-mail: apurba.das@iiti.ac.in

## Table of Contents

1. **Fig. S1.** (a) SEM and (b) TEM images of GQDs shows dots are separated and well distributed.
2. **Fig. S2.** Size distribution profile of GQDs according to TEM image shows the average size of GQDs are nearly about 7-8 nm.
3. **Fig. S3.** SEM image of Gel-F (a) shows microfibrillar network and (b) Gel-Y form nanofibril.
4. **Fig. S4.** TEM image of GQD-Y depicts graphene quantum dots are embedded on fibril (a). And at higher magnification it was shown the size of the decorated GQDs are mostly 7-9 nm. TEM image of GQD-F shows equal distribution of GQDs on the fibril (c), (d).
5. **Fig. S5.** **Fig. S5.** (a) and (b) represent the TEM images at different concentration of GQDs in GQD-F. (a) corresponds to  $0.3 \text{ mg mL}^{-1}$  GQDs shows less amount of GQDs are deposited on the fibril whereas (b) shows more number of GQDs are deposited on the fiber with  $0.7 \text{ mg mL}^{-1}$  of GQDs. (c) and (d) shows the TEM images for GQD-Y with  $0.3 \text{ mg mL}^{-1}$  and  $0.7 \text{ mg mL}^{-1}$  respectively. c and d also showed similar observation as like GQD-F.
6. **Fig. S6.** (a) is the excitation wavelength dependent emission spectra of GQDs.
7. **Fig. S7.** Histogram plot for the error in storage modulus as well as in loss modulus during rheological experiment and all data is from a frequency sweep at 0.1% strain, with values recorded at  $10 \text{ rad s}^{-1}$ .
8. **Fig. S8.** (a), (b) and (c) represent the self-healing property of the gel GQD-Y.
9. **Fig. S9.** FTIR spectrum of synthesized GQDs.
10. **Fig. S10.**  $^1\text{H-NMR}$  spectrum of anthracen-9-ylmethyl (4-nitrophenyl) carbonate **3** in  $\text{CDCl}_3$ .
11. **Fig. S11.**  $^1\text{H-NMR}$  spectrum of Amoc-Phe-OH (**1**) in  $\text{DMSO-d}_6$ .
12. **Fig. S12.**  $^{13}\text{C-NMR}$  spectrum of Amoc-Phe-OH (**1**) in  $\text{DMSO-d}_6$ .
13. **Fig. S13.** ESI-MS spectrum of Amoc-F-OH (**1**).
14. **Fig. S14.**  $^1\text{H-NMR}$  spectrum of Amoc-Tyr-OH (**2**) in  $\text{DMSO-d}_6$ .
15. **Fig. S15.**  $^{13}\text{C-NMR}$  spectrum of Amoc-Tyr-OH (**2**) in  $\text{DMSO-d}_6$ .
16. **Fig. S16.** ESI-MS spectrum of Amoc-Y-OH (**2**).

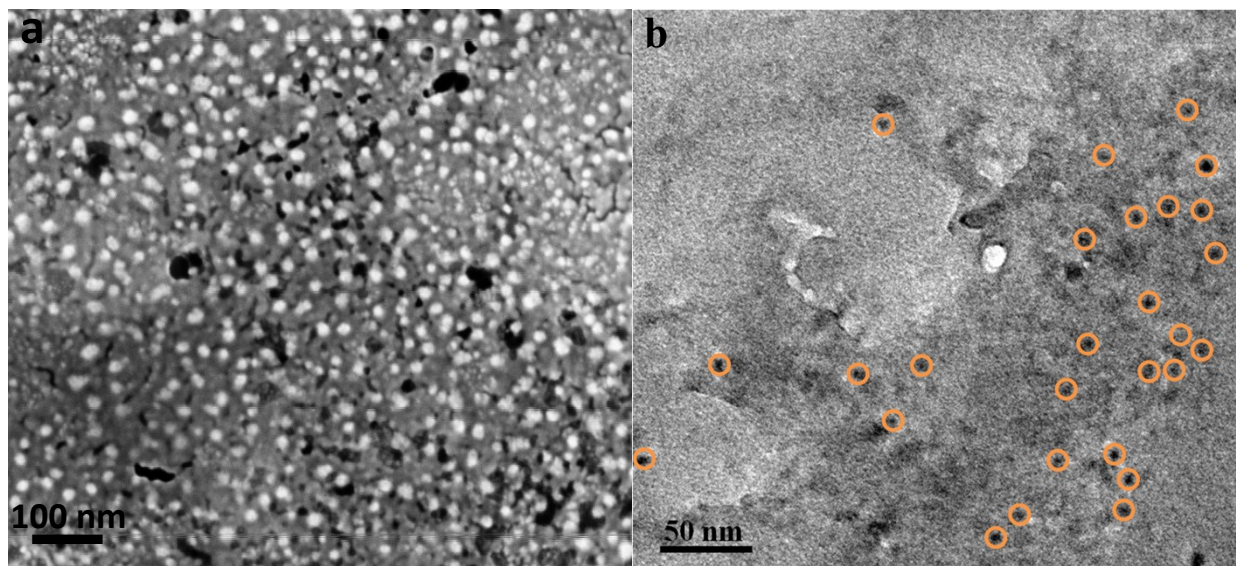


**Fig. S1.** (a) SEM and (b) TEM images of GQDs show dots are separated and well distributed.

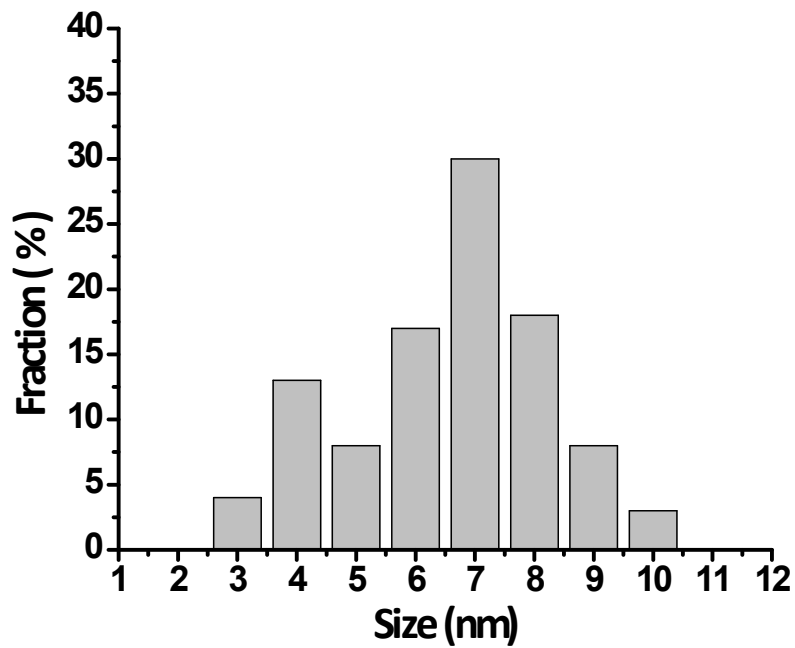


**Fig. S2.** Size distribution profile of GQDs according to TEM image shows the average size of GQDs are nearly about 7-8 nm.

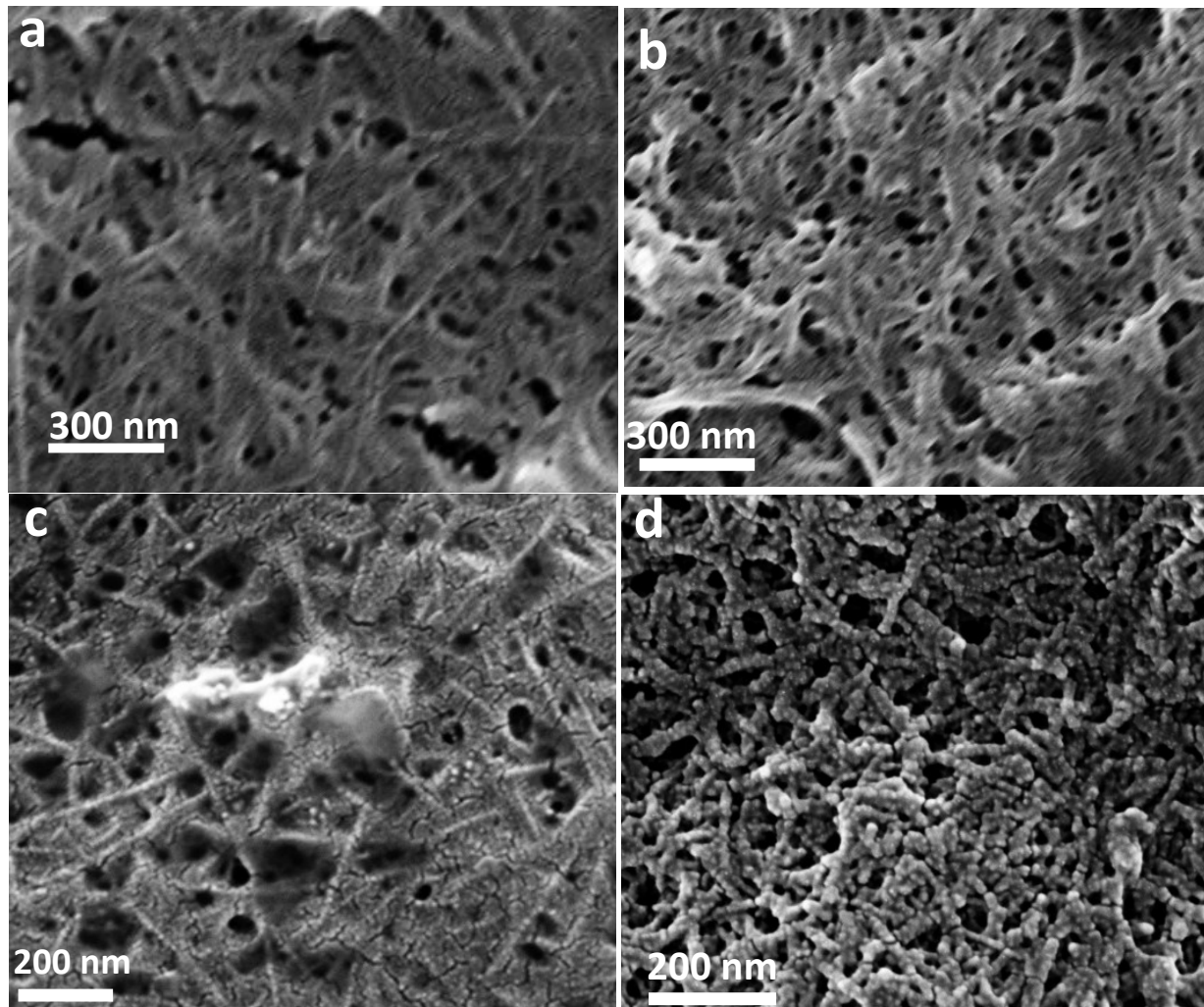


**Fig. S3.** SEM image of Gel-F (a) shows nanofibrillar network. (b) SEM image of Gel-Y shows nanofibrillar network. (c) describe the GQDs decorated morphology by the SEM image of GQD-F (10 mmol L<sup>-1</sup> of Amoc-F-OH with 0.5 mg mL<sup>-1</sup> GQDs) and (d) SEM image shows GQDs deposited fiber of GQD-Y (10 mmol L<sup>-1</sup> of Amoc-Y-OH with 0.5 mg mL<sup>-1</sup> GQDs).

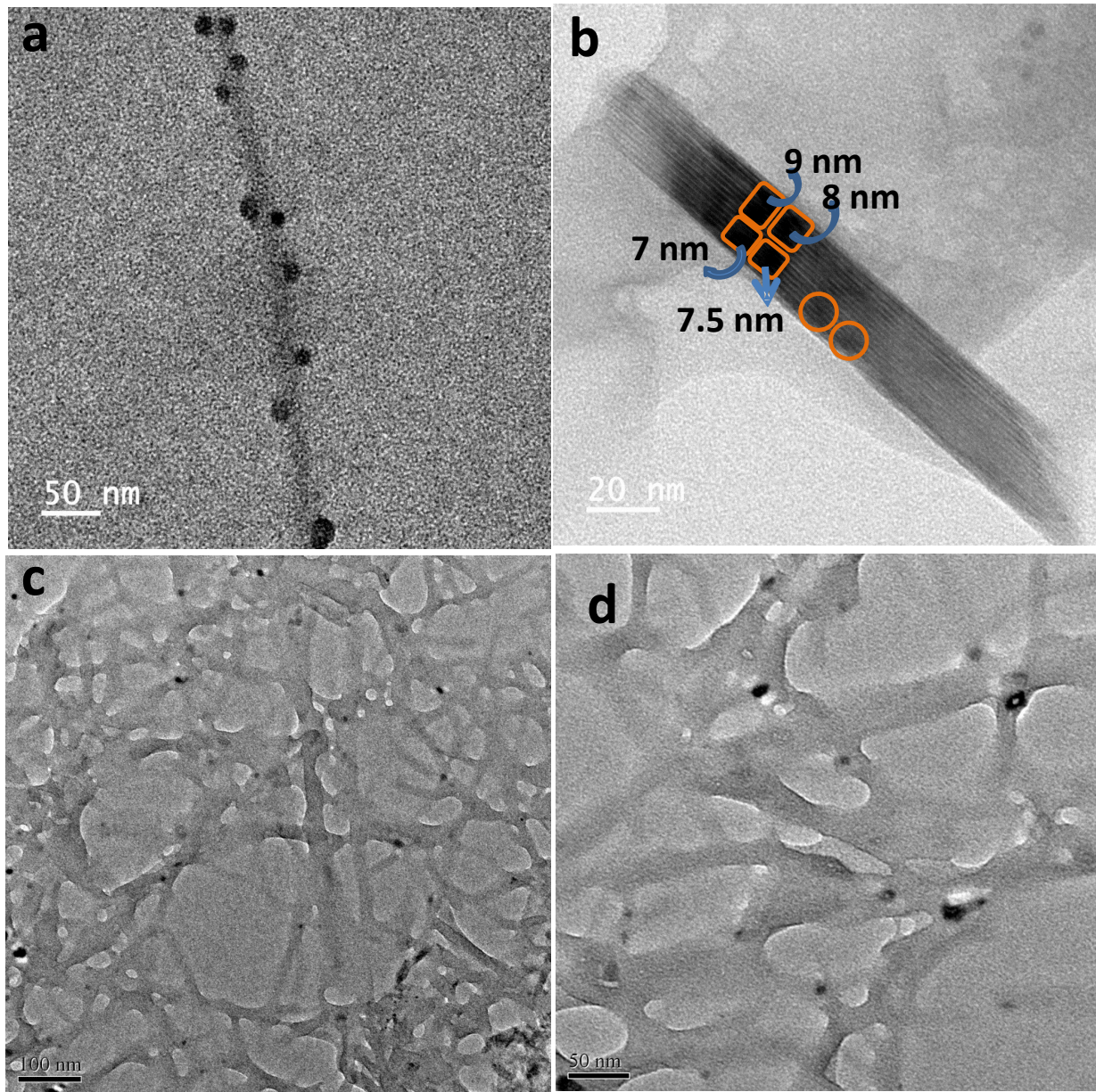


**Fig. S4.** TEM image of GQD-F ( $10 \text{ mmol L}^{-1}$  of Amoc-F-OH with  $0.5 \text{ mg mL}^{-1}$  GQDs) depicts graphene quantum dots are embedded on fibril (a) And at higher magnification it was shown the size of the decorated GQDs are mostly 7-9 nm. (c), (d) TEM images of GQD-Y ( $10 \text{ mmol L}^{-1}$  of Amoc-Y-OH with  $0.5 \text{ mg mL}^{-1}$  GQDs) shows random distribution of GQDs on the fibril.

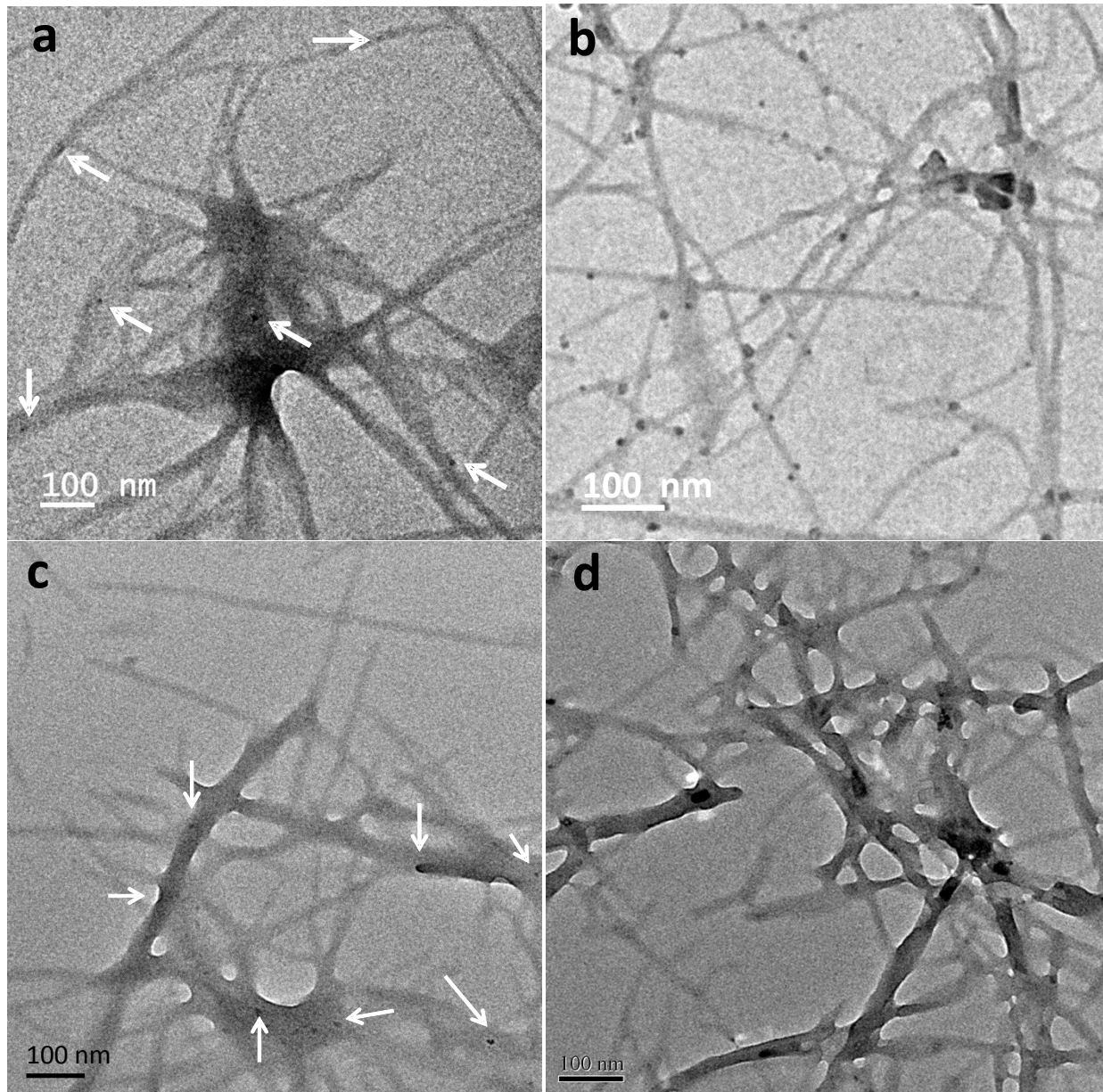


**Fig. S5.** (a) and (b) represent the TEM images at different concentration of GQDs in GQD-F ( $10 \text{ mmol L}^{-1}$  of Amoc-F-OH). (a) corresponds to  $0.3 \text{ mg mL}^{-1}$  of GQDs which shows less amount of GQDs are deposited on the fibril whereas (b) shows more number of GQDs are deposited on the fiber with  $0.7 \text{ mg mL}^{-1}$  of GQDs. (c) and (d) shows the TEM images for GQD-Y with  $0.3 \text{ mg mL}^{-1}$  and  $0.7 \text{ mg mL}^{-1}$  of GQDs respectively. (c) and (d) also showed similar observation as like (a) and (b).

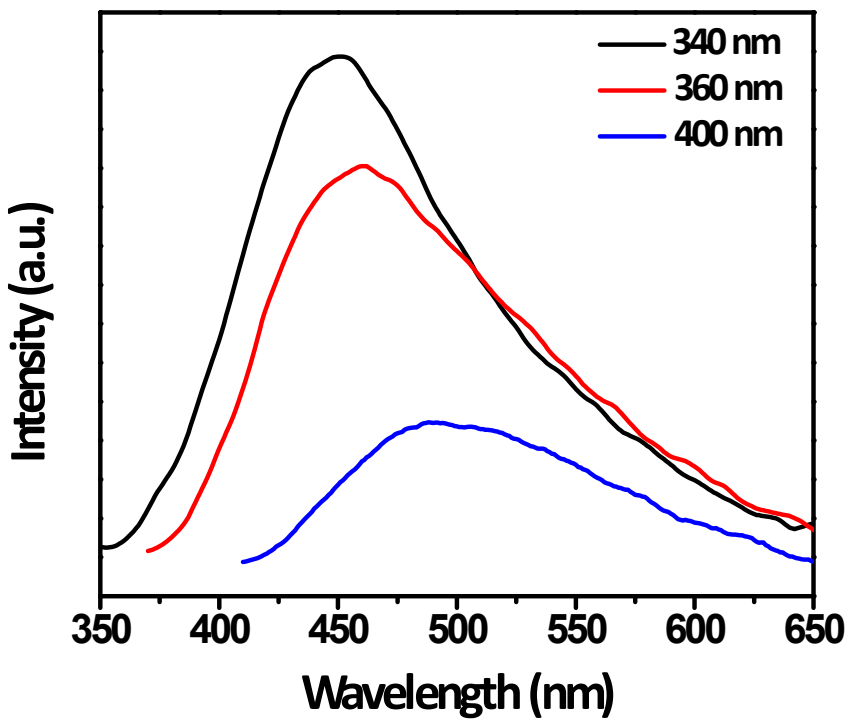


**Fig. S6.** (a) is the excitation wavelength dependent emission spectra of GQDs.

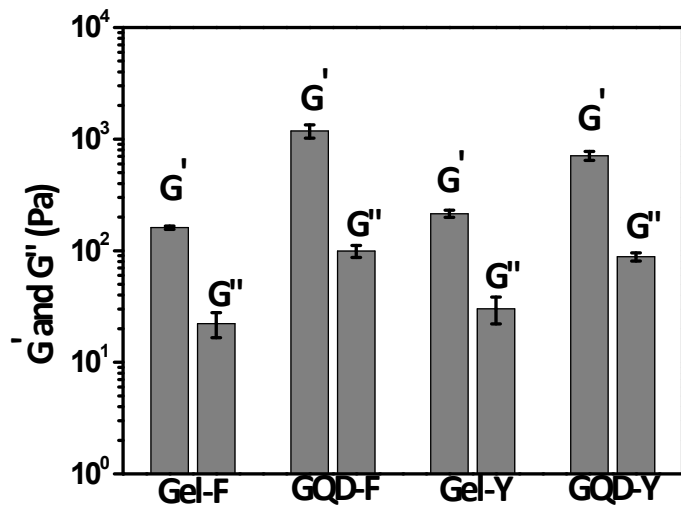


**Fig. S7.** Rheological properties of hydrogels formed using different Amoc-amino acids or composites. All data is from a frequency sweep at 0.1% strain, with values recorded at 10 rad s<sup>-1</sup>.

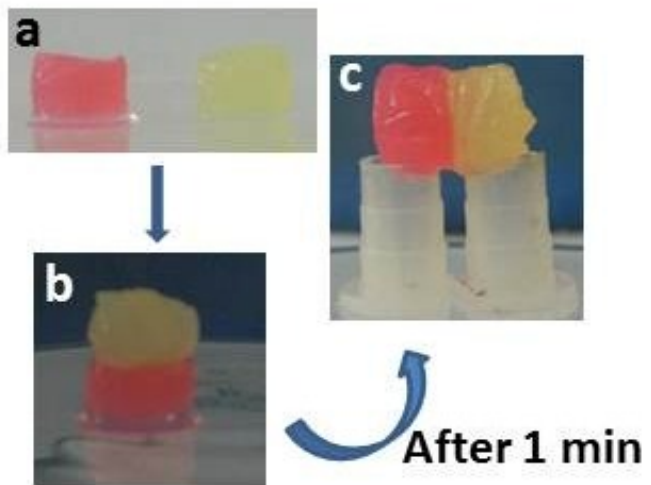


**Fig. S8.** (a), (b) and (c) represent the self-healing property of the gel GQD-Y.

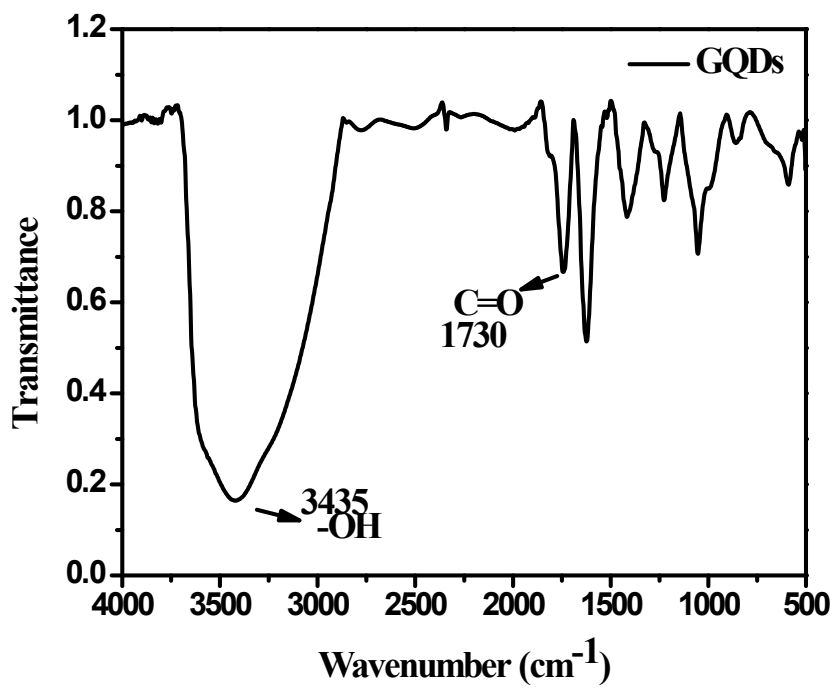


**Fig. S9.** FTIR spectrum of synthesized GQDs.

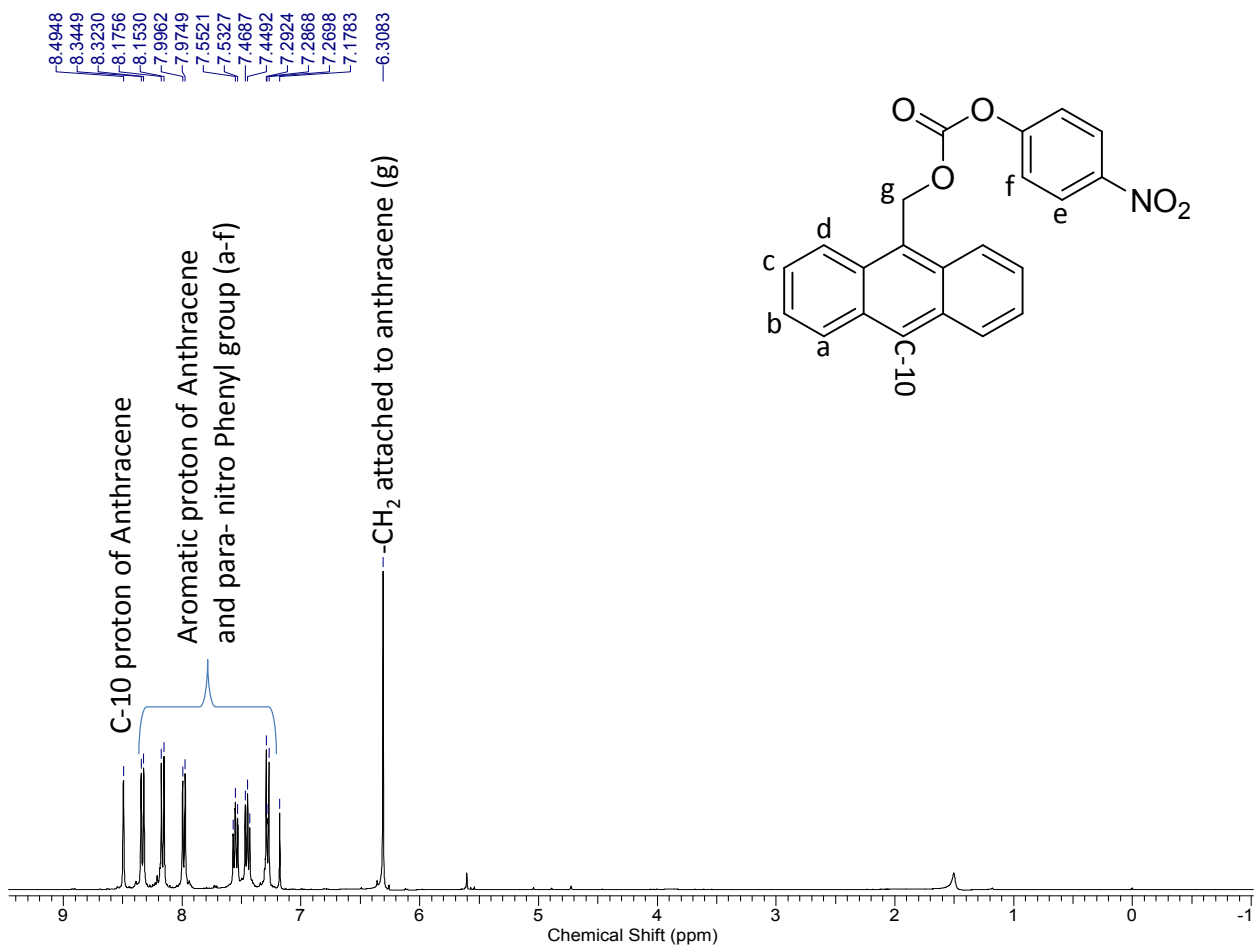


**Fig. S10.** <sup>1</sup>H-NMR spectrum of anthracen-9-ylmethyl (4-nitrophenyl) carbonate **3** in  $\text{CDCl}_3$ .

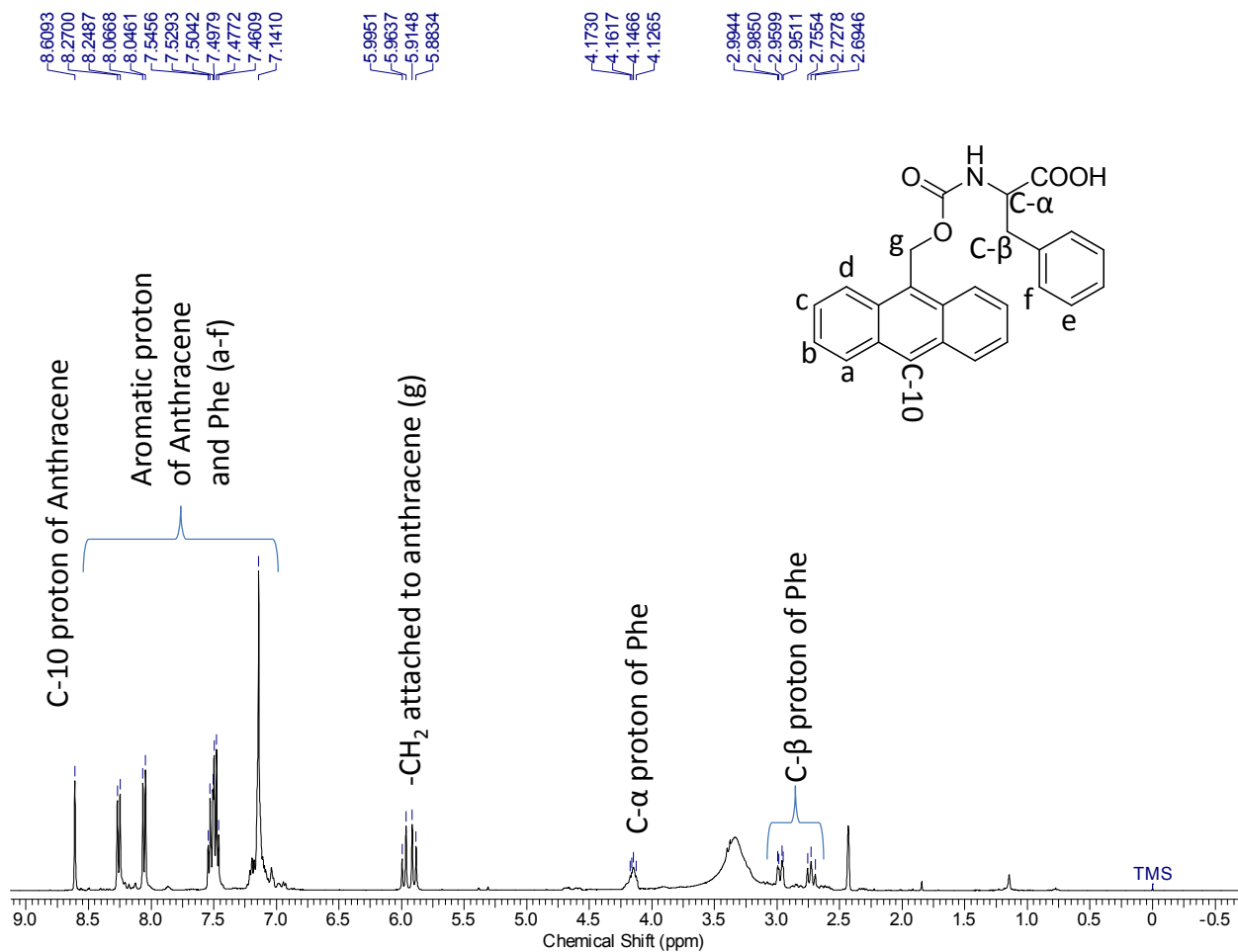


**Fig. S11.**  $^1\text{H}$ -NMR spectrum of Amoc-Phe-OH (**1**) in DMSO- $\text{d}_6$ .

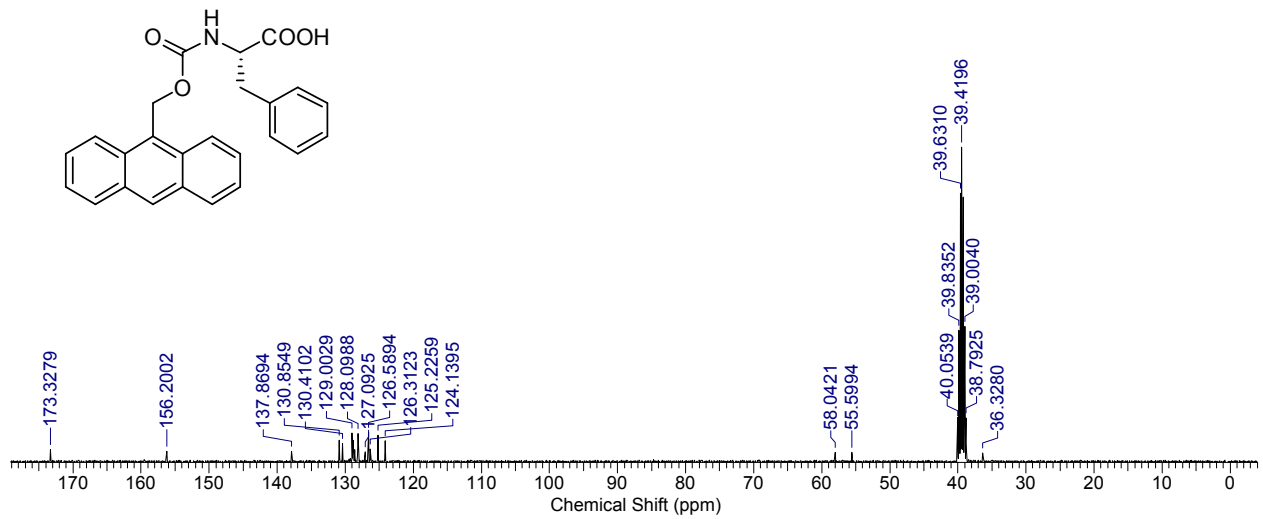


**Fig. S12.**  $^{13}\text{C}$ -NMR spectrum of Amoc-Phe-OH (**1**) in  $\text{DMSO-d}_6$ .

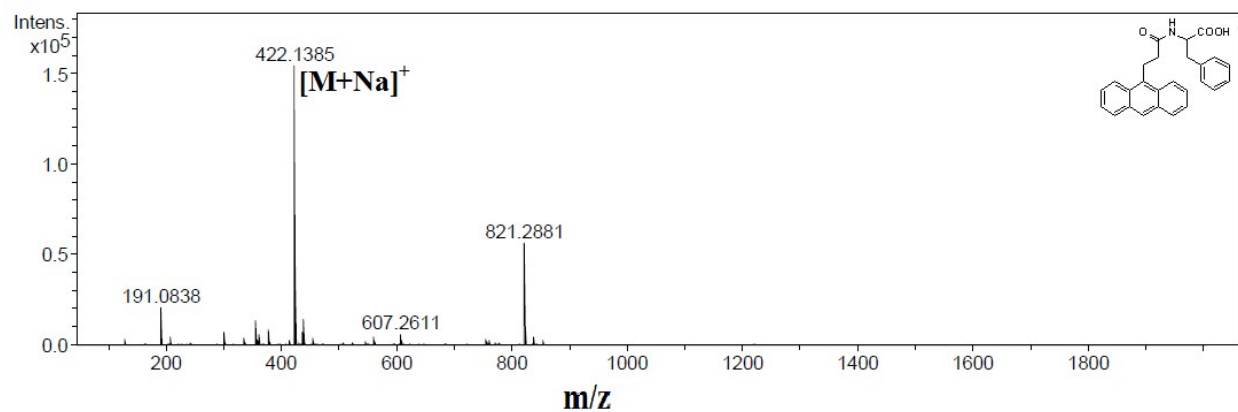


**Fig. S13.** ESI-MS spectrum of Amoc-F-OH (**1**).

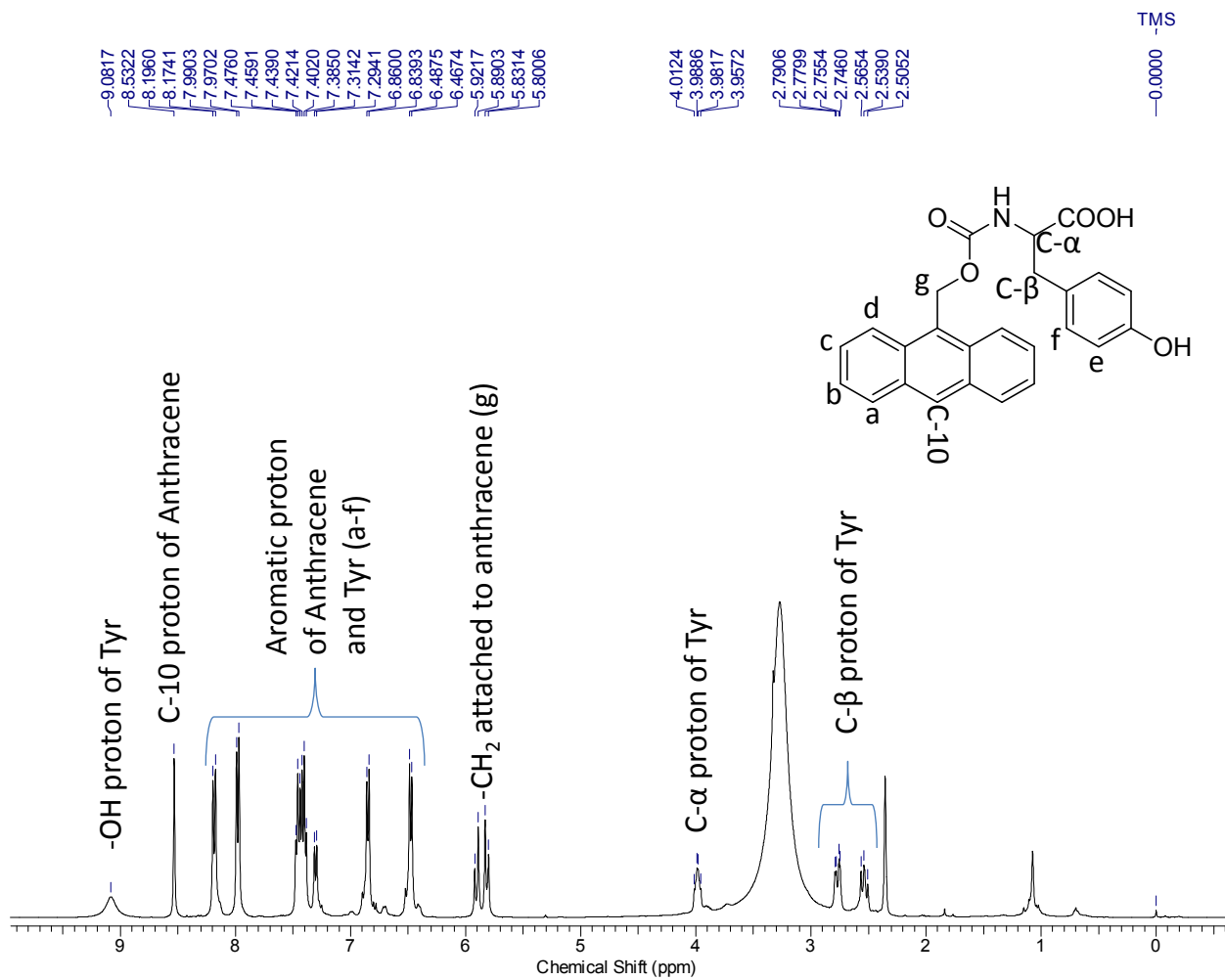


**Fig. S14.**  $^1\text{H}$ -NMR spectrum of Amoc-Tyr-OH (**2**) in  $\text{DMSO-d}_6$ .

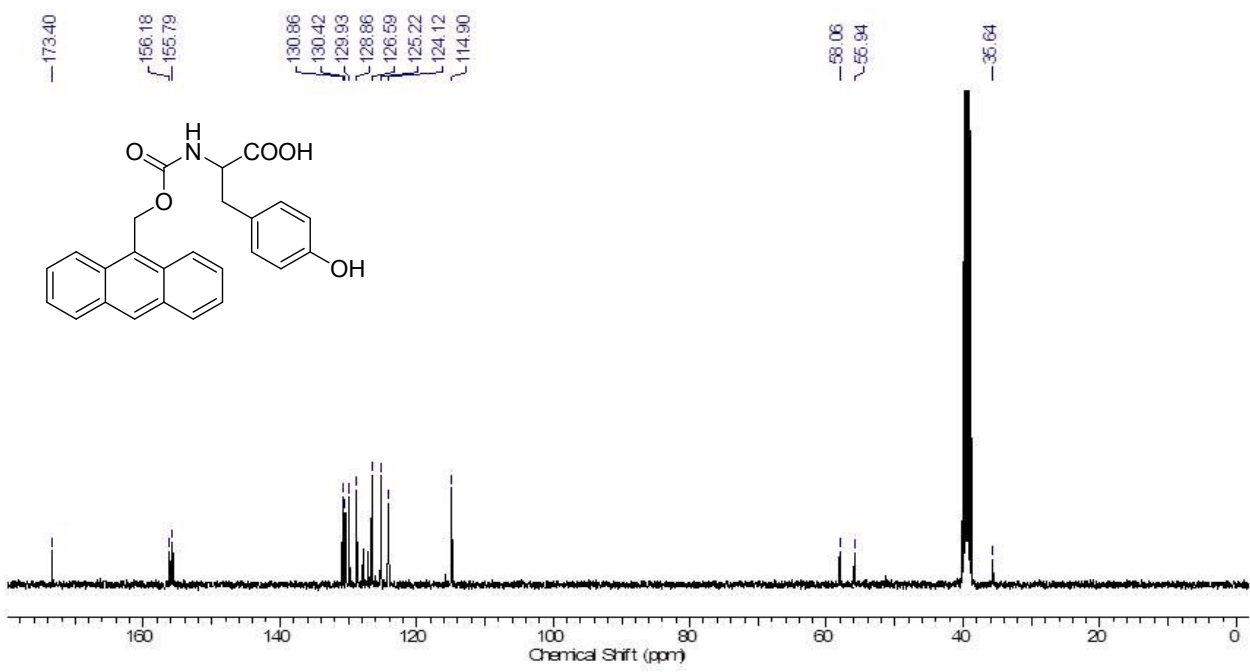


**Fig. S15.**  $^{13}\text{C}$ -NMR spectrum of Amoc-Tyr-OH (**2**) in  $\text{DMSO-d}_6$ .

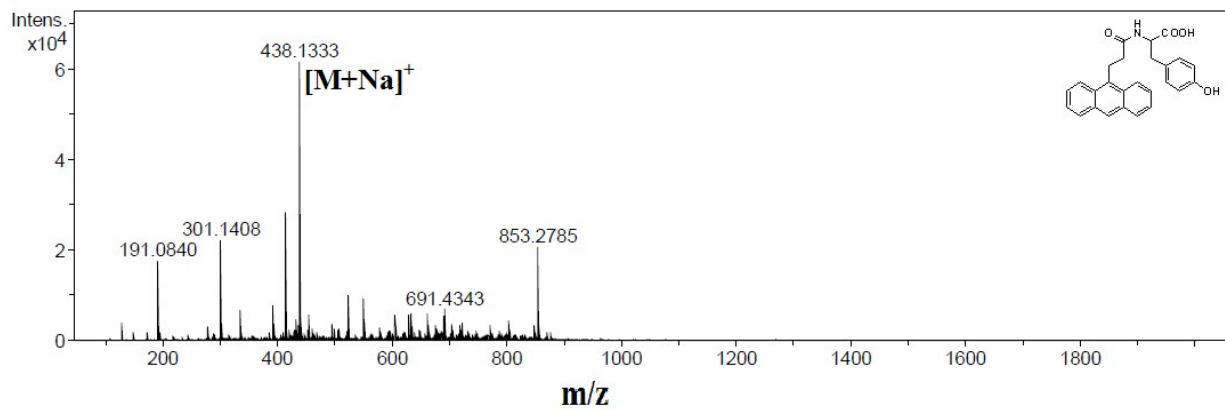


**Fig. S16.** ESI-MS spectrum of Amoc-Y-OH (2).